HHS Public Access

Author manuscript

FASEB J. Author manuscript; available in PMC 2023 February 01.

Published in final edited form as:

FASEB J. 2022 February ; 36(2): e22169. doi:10.1096/fj.202100602R.

Mitochondria modulate ameloblast Ca^{2+} signaling

Veronica Costiniti[1], **Guilherme H. S. Bomfim**[1], **Maria Neginskaya**[1], **Ga-Yeon Son**[1], **Erna Mitaishvili**[1], **Marta Giacomello**[2,3], **Evgeny Pavlov**[1], **Rodrigo S. Lacruz**[1]

[1]Department of Molecular Pathobiology, New York University College of Dentistry, New York, USA

[2]Department of Biology, University of Padova, Padua, Italy

[3]Department of Biomedical Sciences, University of Padova, Padua, Italy

Abstract

The role of mitochondria in enamel, the most mineralized tissue in the body, is poorly defined. Enamel is formed by ameloblast cells in two main sequential stages known as secretory and maturation. Defining the physiological features of each stage is essential to understand mineralization. Here, we analyzed functional features of mitochondria in rat primary secretory and maturation stage ameloblasts focusing on their role in Ca^{2+} signaling. Quantification of Ca^{2+} stored in mitochondria by FCCP stimulation was comparable in both stages. The release of endoplasmic reticulum Ca^{2+} pools by ATP in rhod2AM loaded cells showed similar $_{m}Ca^{2+}$ uptake. However, $_{m}Ca^{2+}$ extrusion via NCLX was more prominent in maturation. To address if $_{m}Ca^{2+}$ uptake via the mitochondrial Ca^{2+} uniporter (MCU) played a role in $_{c}Ca^{2+}$ buffering, we stimulated Ca^{2+} influx via the store operated Ca^{2+} entry (SOCE) and blocked MCU with the inhibitor Ru265. This inhibitor was first tested using the enamel cell line LS8 cells. Ru265 prevented $_{c}Ca^{2+}$ clearance in permeabilized LS8 cells like ruthenium red, and it did not affect $\Delta\Psi m$ in intact cells. In primary ameloblasts, SOCE stimulation elicited a significantly higher $_{m}Ca^{2+}$ uptake in maturation ameloblasts. The uptake of Ca^{2+} into the mitochondria was dramatically decreased in the presence of Ru265. Combined, these results suggest an increased mitochondrial Ca^{2+} handling in maturation but only upon stimulation of Ca^{2+} influx via SOCE. These functional studies provide insights not only on the role of mitochondria in ameloblast Ca^{2+} physiology, but also advances the concept that SOCE and $_{m}Ca^{2+}$ uptake are complementary processes in biological mineralization.

Keywords

Enamel; secretory; maturation; mitochondria; MCU

Correspondence: Rodrigo S. Lacruz, Department of Molecular Pathobiology, New York University College of Dentistry. 345 East 24th street, New York, NY 10010, USA. rsl10@nyu.edu.

7.AUTHORS CONTRIBUTIONS

V. Costiniti, R.S. Lacruz and M. Giacomello designed the research studies. V. Costiniti, G.H.S. Bomfim, M. Neginskaya, G.Y. Son and E. Mitaishvili performed the experiments. V. Costiniti, M. Giacomello, E. Pavlov and R.S. Lacruz analyzed the data. V. Costiniti, R.S. Lacruz, M. Giacomello and E. Pavlov wrote the paper. All authors contributed to the final preparation of the manuscript.

6.CONFLICT OF INTEREST

The authors declare no conflict of interest.

1. INTRODUCTION

Specialized ectodermal cells known as ameloblasts secrete a unique matrix that they help mineralize during the stages of secretory and maturation. The physiological events involved at each stage control enamel mineralization in fundamental ways. Secretory ameloblasts provide a proteinaceous organic template for the elongating enamel crystals to grow, and maturation ameloblasts provide increased ion transport and engage in protein removal allowing crystals to expand in width and thickness (1-3). Ca^{2+} participates in enamel formation at several levels: Ca^{2+} is an abundant and essential component of mineralized enamel crystals (1, 4) and is also a second messenger in ameloblasts signaling modulating the expression of important enamel-specific genes (5-8). Recent advances in ameloblast physiology showed that Ca^{2+} uptake into the ameloblasts is regulated by the store operated Ca^{2+} entry (SOCE) pathway (5, 6, 9, 10). SOCE is mediated by the endoplasmic reticulum (ER) resident Ca^{2+} sensors stromal interacting molecule (STIM1 and STIM2) that activate the highly specialized Ca^{2+} channel ORAI in the plasma membrane (11-14). Stimulation of SOCE in rat ameloblasts showed significantly higher cytosolic Ca^{2+} ($_cCa^{2+}$) uptake in maturation cells compared to the secretory ameloblasts (5, 6, 15). We suggested that SOCE is important to provide a Ca^{2+} supply to the ameloblasts as a critical step for its vectorial transport providing the growing enamel crystals with this fundamental mineralizing agent (6, 16-19). We have also suggested that elevations in $_cCa^{2+}$ controlled by SOCE likely participate in additional ameloblast functions (19). In SOCE-deficient mice, the ameloblasts have poor Ca^{2+} uptake and the enamel is hypomineralized (9, 10). Surprisingly, the ameloblasts of these mice showed abnormal mitochondrial morphology and mitochondrial function was also affected (10). In addition, a murine enamel cell line with a knock-down of *Orai1* showed alterations in mitochondrial respiration and cell redox state (9). These data suggest important connections between Ca^{2+} uptake, mineral growth and mitochondria in ameloblasts. It also underscores the possibility that mitochondria in ameloblasts may play a role in Ca^{2+} signaling because mitochondria are known to shape Ca^{2+} transients in cells by modulating SOCE (20-22). However, the function of mitochondria in ameloblasts is poorly defined (23).

Mitochondria regulate cellular metabolism controlling oxidative phosphorylation (OXPHOS) and ATP production, a process that requires the presence of Ca^{2+} in the mitochondrial matrix to activate Ca^{2+} sensitive dehydrogenases (24, 25). Mitochondria are also important $_cCa^{2+}$ buffers contributing to signaling events in cells (26-32). The main route for Ca^{2+} uptake into the mitochondria is via the mitochondrial Ca^{2+} uniporter (MCU) complex, a Ca^{2+}channel expressed in the inner mitochondrial membrane, a process facilitated by the steep membrane potential ($\Delta\Psi m$) of the mitochondria (33-36). The activation of the MCU channel requires an increase in the concentration of $_cCa^{2+}$ well above basal levels, and its activity is modulated by several factors including MICU1-2, MCUb, MCUR1, and EMRE (37-44). Mitochondrial Ca^{2+} ($_mCa^{2+}$) is also influenced by the proximity of mitochondria to the ER, the main intracellular Ca^{2+} store of the cell (45), $_mCa^{2+}$ extrusion is modulated by the Na^+-Li^+-Ca^{2+} exchanger NCLX (46) and possibly the Ca^{2+}/H^+ antiporter LETM1 (38), although the latter remains contentious (47).

The role of mitochondria in bone mineralization has been appreciated for decades, by contrast, mitochondrial function in enamel formation has remained poorly defined despite that enamel is much more calcified than bone. The enamel studies have largely focused on morphological analysis and subcellular localization of the mitochondria in the ameloblasts, and the identification of mitochondrial enzymes (48-50), but there is an overwhelming dearth of functional studies. To gain a better understanding of the physiological role of mitochondria in enamel formation, we recently analyzed OXPHOS levels in ameloblasts and showed that this function was upregulated in maturation (51). A recent report confirmed the important role of OXPHOS in mice with impaired mitochondrial DNA (mtDNA) replication which showed abnormal enamel (52). Because $_{m}Ca^{2+}$ handling is important for the activation of OXPHOS and ATP production (25, 28, 53), here we have addressed the Ca^{2+} handling role of mitochondria in ameloblasts. We show that the mitochondria of secretory and maturation ameloblasts store a similar quantity of Ca^{2+} in the matrix and that Ca^{2+} released from the ER by agonist-stimulation is equally captured by mitochondria of both cell types. We show that SOCE activation results in significantly higher $_{m}Ca^{2+}$ uptake by the mitochondria of maturation stage ameloblasts, and that this process involves MCU. These data provide an important step toward understanding the role of mitochondria in enamel by addressing not only its impact in ameloblast Ca^{2+} physiology, but also advances the concept that SOCE and $_{m}Ca^{2+}$ uptake are complementary processes in biological mineralization.

2. MATERIALS AND METHODS

2.1. Animals:

All animal procedures were conducted in accordance with the guidelines approved by the Institutional Animal Care and Use Committee (IACUC) of New York University College of Dentistry (protocol # s16-00625).

2.2 Cell cultures

For primary enamel cell cultures, the lower incisors of Sprague Dawley rats (~100 gr) were collected to isolate primary secretory and maturation enamel organ cells as described (5, 10). Because the number of cells isolated from the enamel organ of a single animal is low (54), we pool cells from at least 2 rats for each experiment. This procedure allows us to analyze technical triplicates. The isolated enamel organ was incubated with Liberase (0.25 mg/ml; Roche) for 30 min at 37 °C then trypsinized (Trypsin; Gibco) for 10 min at 37 °C. They were plated onto Cell-Tak (Corning) coated plates or coverslips in X-Vivo15™ medium (Lonza) supplemented with 10 % FBS (Thermo Fisher Scientific) and 1 % penicillin/ streptomycin (Thermo Fisher Scientific). Isolated ameloblasts were used within 24 h after dissection. The purity of the dissection was validated by RT-qPCR of specific enamel genes for the two stages (*Enam* and *Odam* for the secretory and maturation stages, respectively) (Fig. S1A) and by Western blot of the enamel matrix protein Amelogenin (Fig. S1B), which is primarily translated in the secretory enamel stage. Fibroblasts were detected by either FITC fluorescent or PE anti-rat CD90/mouse CD90.1 (Thy-1.1) (1:500, 30 min at 37 °C; BioLegend), as we have reported previously (23).

The murine ameloblast LS8 cell line (55) was used to address the effects of the MCU blockers Ruthenium 265 (Ru265) and Ruthenium Red (RuR). Cells were plated onto Poly-L-lysine (Sigma) coated plates or coverslips in DMEM medium (Lonza) supplemented with 10 % FBS (Thermo Fisher Scientific) and 1 % penicillin/streptomycin (Thermo Fisher Scientific). Cells were used within 24 to 48 h after plating.

2.3 Real time PCR (RT-qPCR)

Total RNA was isolated using the RNeasy Mini Kit (Qiagen # 217004) as indicated by the manufacturer followed by reverse transcription using the iScript cDNA Synthesis Kit (Biorad). For mRNA quantification we used the SsoAdvanced Universal SYBR Green qPCR Supermix (BioRad) and performed the experiments in a CFX Connect Thermocycler (BioRad). Primers were used at a concentration of 0.25 nM with β-*Actin* functioning as the housekeeping gene. Relative quantification of gene expression was determined by the $2^{-\Delta\Delta CT}$ method. Table 1 lists all primers used.

2.4 NCLX activity measurements

Ameloblasts were plated per well onto 384-well plates (CellCarrier, PerkinElmer). Cells were rinsed in 10 mm HEPES buffered saline (HBSS buffer, pH 7.4; Thermo Fisher Scientific), subsequently loaded with 1 μM fluo3AM or 4 μM rhod2AM (30 min at 37 °C; Thermo Fisher Scientific) in absence/presence of the NCLX inhibitor CGP-37157 (30 min at 37 °C 10 μM; SantaCruz) and washed before image acquisition. Alternate brightfield, digital phase contrast, 488 and 580 fluorescence (excitation/emission at: 460-490/ 500-550; 520 – 552/581 – 630 nm, respectively) images were acquired every 15 seconds, using the 20X magnification air objective of the high content screening imaging system Operetta® and Harmony® software (PerkinElmer). 100 μM ATP (Sigma) was added after 2 min in absence of Ca^{2+} (EGTA 100 μM) to induce ER Ca^{2+} release. Analysis was performed by means of Harmony® software (PerkinElmer) as follows. Image segmentation was performed by Region of Interest in the Digital Phase contrast channel. Ca^{2+} dyes fluorescence intensity was calculated per each individual cell, and background corrected. Dyes fluorescence intensity, background corrected, was then measured per each region of interest (that is, per each individual cell) and averaged.

2.5 Quantification of $_cCa^{2+}$ and $_mCa^{2+}$

To simultaneously record $_cCa^{2+}$ and $_mCa^{2+}$, LS8 cells and primary ameloblasts were loaded with 1 μM fluo4AM (ThermoFisher Scientific) and 4 μM rhod2AM (30 min at room temperature; ThermoFisher Scientific). To quantitate $_cCa^{2+}$, cells were loaded with 1 μM fura2AM (1 h at room temperature; ThermoFisher Scientific) in Ca^{2+} containing Ringer's solution [2 mM Ca_2Cl, 155 mM NaCl, 4.5 mM KCl, 3 mM MgCl2, 5 mM Na-Hepes, and 10 mM d-glucose (pH 7.4)]. To induce mitochondrial Ca^{2+} release 1 μM protonophore FCCP (Trifluoromethoxy carbonylcyanide phenylhydrazone; Sigma) (56) was added after 2 - 5 min in presence of 2 mM Ca^{2+}. To stimulate ER Ca^{2+} release, ameloblasts were treated with 100 μM ATP in free Ca^{2+} ringer solution (EGTA 100 μM). SOCE activity was stimulated by pre-incubation with 2 μM thapsigargin (20 min; Sigma), placed in free Ca^{2+} ringer solution and then perfused with ringer solution containing 2 mM Ca^{2+}. Fluorescence intensities were recorded every 3 to 5 s after excitation using the 20X magnification air objective on a

Nikon 2000 U Eclipse microscope. The ratio F_{340}/F_{380} of fura2AM values, the fluo4AM and rhod2AM fluorescence intensity, background corrected, were measured per each region of interest using Nikon ND software.

2.6. Mitochondrial depolarization

To quantitate mitochondrial depolarization, we used the cell-permeant dye TMRM (tetramethylrhodamine methyl ester) which accumulates in active mitochondria with intact membrane potential. 10 K LS8 cells were plated per well onto 96-well plates (Grainger). After 24 h in culture, cells were rinsed in HEPES buffered saline (HBSS buffer, pH 7.4; Thermo Fisher Scientific) and subsequently loaded with 40 nM TMRM (ThermoFisher Scientific) in HBSS in the presence of 1 μM cyclosporine H (30 min at 37 °C; Santa Cruz) which was maintained during image acquisition. Cells were treated with 1 μM oligomycin A at 5 min to inhibit the ATP synthase and induce hyperpolarization of the mitochondrial membrane potential. 1 μM FCCP was added at 25 min as a control for mitochondrial depolarization as it provokes the $\Delta\Psi m$ collapse and the consequent TMRM discharge from mitochondria (57). The fluorescence was detected for 40 min (excitation/emission at: 520 – 550/560 – 630 nm) in a Flexstation 3 plate reader (Molecular Devices) acquiring the signal every 60 sec. The fluorescence intensity of each analyzed well was plotted against time.

2.7 Ca^{2+} retention capacity assay in permeabilized cells

LS8 cells were plated on 6-well plates (200 K cells per well). After 24 h, they were detached by adding 250 μl Trypsin-EDTA 0.25% (Gibco). Cells were collected in extracellular medium 1 ml [2% bovine serum albumin (Sigma), 121 mM NaCl, 5 mM $NaHCO_3$, 10 mM Na–Hepes, 4.7 mM KCl, 1.2 mM KH_2PO_4, 1.2 mM $MgSO_4$, 2 mM $CaCl_2$ and 10 mM glucose, (pH 7.4)] (58) and centrifuged for 5 min at 1000 rpm and supernatants were discarded. Pellets were re-suspended in 1 mL of intracellular medium [120 mM KCl, 10 mM NaCl, 1 mM KH_2PO_4, 2 mM $MgCl_2$, 20 mM HEPES – KOH, 2 mM succinate, 2 μM rotenone, EGTA 5 μM, thapsigargin 2 μM] containing 1 μM Calcium Green-5 N (58, 59). We added 40 μM digitonin (100 s) to the intracellular medium to permeabilize the cells, then 5 μM RuR or Ru265 were added (300 s) to block mitochondrial Ca^{2+} uptake. Successive accumulative additions of 20 μM Ca^{2+} boluses were added to the cuvettes containing the cells, while measuring the fluorescence in the spectrometer. Fluorescence was measured using a Perkin Elmer LS55 Luminescence Spectrometer, set up at 506 nm for emission, 480 nm for excitation, and with 2.5 mm slits for both, emission and excitation.

2.8 Western blot analysis

Total lysates of primary secretory and maturation enamel cells were prepared in Ripa Buffer (Thermo Fisher Scientific), Protease cocktail inhibitor 100X (Thermo Fisher Scientific), Laemli buffer 4X (BioRad) and β-mercaptoethanol (BioRad) and then loaded at the concentration of 5 μg in 10% SDS-polyacrylamide resolving gels (BioRad). Lysates of HEK-293 cells were prepared as above and used as a negative control. Nitrocellulose membranes were saturated with fat-free milk 5% in TBS (Tris-HCl 50 mM, NaCl 150 mM, pH 7.5) Tween 0.1% for 1 h at room temperature and probed with antibodies against Amelogenin (AMELX, Santa Cruz Biotechnology, sc-32892) and β-Actin (Santa Cruz Biotechnology, sc-47778). Signals were amplified and visualized with horseradish

peroxidase-conjugated secondary antibody (Bio-Rad) and enhanced chemiluminescence detected by the Bio-Rad ChemiDoc gel documentation setup. Images of the acquired Western blots were analyzed using the ImageJ software.

2.9 Statistics

All statistical analyses of the data were done using Prism9 (GraphPad Software). A minimum of three independent experiments were performed. The Δ, peak, slope and [Ca^{2+}] (area under the curve) were calculated by integrating the transients versus time during the stimulus duration for each experiment. The slope parameter was fitted by the GraphPad Prism software using the one-phase association equation. Difference between the means of the group data that fit a normal distribution were analyzed using one-way ANOVA, followed by a Bonferroni's multiple comparison post-hoc test, or analyzed by a two-tailed unpaired Student's t-test. Differences with p values of < 0.05 were considered significant: * $p<0.05$, ** $p<0.01$ and ***$P < 0.001$. Results are shown as means ± SEM of minimum three independent experiments.

3. RESULTS

3.1 Ca^{2+} stored in mitochondria is comparable across stages

The mitochondrial matrix functions as an important Ca^{2+} storage (24, 28, 60, 61) with Ca^{2+} reversibly complexed with P_i forming $Ca_3(PO_4)_2$ (62) maintaining a low $_mCa^{2+}$ concentration (63). To investigate whether the amount of Ca^{2+} stored in the mitochondria of secretory and maturation ameloblasts differs, we stimulated fura2AM loaded secretory and maturation stage ameloblasts with the protonophore FCCP which uncouples OXPHOS collapsing the $\Delta\Psi m$ and releasing $_mCa^{2+}$ into the cytosol (56). Using this approach, we showed that there were no statistically significant differences between stages (Fig. 1A-B). We then repeated the same experiment but loading the cells with the mitochondrial Ca^{2+} indicator rhod2AM, and we showed that FCCP stimulation elicited a similar decay of rhod2AM fluorescence intensity in both cell types (Fig. 1C-D). These data indicate that the quantity of Ca^{2+} stored in the mitochondria of both cell types is comparable.

3.2 Similar ER-Mitochondrial Ca^{2+} transfer

Mitochondria are often strategically located near the ER allowing the mitochondria to capture a substantial fraction of the Ca^{2+} released by the ER (20). We loaded ameloblasts with the mitochondrial Ca^{2+} indicator rhod2AM and stimulated ER Ca^{2+} release by ATP to quantitate $_mCa^{2+}$ uptake in the absence of external Ca^{2+}. Extracellular ATP is widely known to stimulate the release of Ca^{2+} pools from the ER (64, 65), including the ameloblasts (6). Our results show that the mitochondria of both ameloblast types capture the ER Ca^{2+} pools released by ATP, and we show that secretory and maturation ameloblasts do so equally (Fig. 1E-F).

3.3 $_mCa^{2+}$ extrusion via NCLX is more prominent in maturation

The electrogenic exchanger NCLX is considered the main carrier extruding Ca^{2+} out of the mitochondria (46, 47). We analyzed the expression of *Nclx (Slc8b1)* in rat secretory and maturation and showed that its mRNA is upregulated in maturation (Fig. 2A). We

then tested NCLX function using the NCLX inhibitor CGP-37157 (66). We first assessed if CGP-37157 (10 μM) affected $_{c}Ca^{2+}$ in ameloblasts but this was not the case (Fig. S2). To analyze $_{m}Ca^{2+}$ clearance, we loaded secretory and maturation stage ameloblasts with rhod2AM and stimulated the cells with ATP, which, as shown above, induces $_{m}Ca^{2+}$ uptake. Upon CGP-37157 pre-treatment, maturation ameloblasts showed higher $_{m}Ca^{2+}$ (Fig. 2B-C), suggesting that blocking NCLX leads to the increased accumulation of Ca^{2+} in the matrix and therefore NCLX mediated $_{m}Ca^{2+}$ clearance is a more prominent function during the maturation stage.

3.4 Pharmacological effects of the MCU blocker Ru265 in enamel cells.

To address the role of MCU in $_{m}Ca^{2+}$ uptake in enamel cells more directly, we used the recently described cell permeable MCU inhibitor Ru265 (67). This compound was reported to inhibit MCU by binding to the DIME-Asp, D261, in the transmembrane helix TMH2 at the cytoplasmic facing entrance of the pore (68). First, we tested several concentrations (1 μM, 10 μM, 20 μM, 50 μM) of this inhibitor in the murine enamel line LS8 cells that are widely used in enamel research [55, 69] (Fig. 3A-C). In rhod2AM loaded LS8 cells, we showed that 50 μM of Ru265, as previously reported [67], was the most efficient concentration in blocking $_{m}Ca^{2+}$ uptake (Fig. 3A-C). We also showed that the clearance of extramitochondrial Ca^{2+} of digitonin-permeabilized LS8 cells after the addition of Ca^{2+} boluses (20 μM) in the presence of Ru265 was dramatically hindered (Fig. 3D). Similar results were obtained by pretreating the LS8 cells with the better known MCU blocker RuR, in the same conditions (Fig. 3D). Because these experiments were performed in the presence of the irreversible SERCA inhibitor thapsigargin, the effect of Ru265 on preventing Ca^{2+} clearance is independent of the SERCA mediated ER Ca^{2+} refilling. To further investigate if Ru265 affected mitochondrial membrane potential in enamel cells, we pretreated the LS8 cells loaded with the mitochondrial membrane potential indicator TMRM (40 nM) and with Ru265 (50 μM) and showed that this had no effect on ΔΨm (Fig. 3E). These data confirms that Ru265 blocks $_{m}Ca^{2+}$ uptake without affecting ΔΨm.

3.5 $_{m}Ca^{2+}$ uptake is higher in maturation ameloblasts

The MCU complex is formed by the channel pore MCU, in the inner mitochondrial membrane, together with several regulators that positively (MICU1, MICU2, MCUR1) or negatively (MCUb) modulate the channel (41, 43, 44, 70). We tested differences in gene expression of *Mcu* and its modulators in rat secretory and maturation ameloblasts and found no differences in their expression except for the positive MCU regulator MCUR1, which was upregulated in the maturation stage (Fig. 4A). We also tested the expression of the main components of SOCE, STIM1, STIM2 and ORAI1, as well as the possible SOCE modulator TRPC1 (71). The expression of *Stim1, Stim2, Orai1* and *Trpc1* in rat enamel organs was upregulated in maturation (Fig. 4B) further confirming the fundamental role of SOCE in maturation primary ameloblasts (5, 19). Secretory and maturation cells were loaded with the non-ratiometric indicators fluo4AM and rhod2AM to simultaneously quantitate $_{c}Ca^{2+}$ and $_{m}Ca^{2+}$ uptake, respectively, in the presence/absence of Ru265 (50 μM) (67). Stimulating SOCE elicited a substantial increase in $_{c}Ca^{2+}$ with higher levels in maturation (Fig. 4C, D), supporting our previous reports using fura2AM (5, 6, 15). We also observed that $_{m}Ca^{2+}$ uptake replicated these changes in $_{c}Ca^{2+}$ because there was a significantly higher uptake

of Ca^{2+} into the mitochondrial matrix of maturation cells (Fig. 4E-H). The slope of $_{m}Ca^{2+}$ uptake, indicative of the rate of uptake (Fig. 4H) and the total amount of Ca^{2+} entering the mitochondria in maturation ameloblasts were significantly higher in maturation (Fig. 4F, G). In the presence Ru265, $_{m}Ca^{2+}$ uptake was significantly decreased in both cells indicating that it was mediated by MCU (Fig. 4E-H).

4. Discussion

Mitochondria have been associated with biological mineralization for decades, largely in the context of bone (72-75). By contrast, the role of mitochondria in enamel, the most mineralized tissue in vertebrates, is poorly understood. We probed the mitochondria of secretory and maturation stage ameloblasts to analyze their role in Ca^{2+} physiology and to test whether there are differences in $_{m}Ca^{2+}$ dynamics between these cell types.

First, we investigated differences in the Ca^{2+} stored in the mitochondria of both cell types. By stimulating the release of $_{m}Ca^{2+}$ with FCCP, we showed a similar decline in rhod2AM fluorescence and a comparable increase in fura2AM signals between cell types, suggesting that there were no significant differences in the amount of Ca^{2+} accumulated in the mitochondria of secretory or maturation ameloblasts. We next focused our attention on the potential differences in the Ca^{2+} exchange between the ER and the mitochondria. Releasing ER Ca^{2+} pools by ATP stimulation, which we have previously shown as an effective strategy in ameloblasts (6), also showed a comparable amount of $_{m}Ca^{2+}$ uptake in both cell types. As $_{m}Ca^{2+}$ uptake is balanced by Ca^{2+} extrusion via NCLX, the main exchanger mediating $_{m}Ca^{2+}$ release (76), we investigated if the exchanger showed differences it its activity in both cells. The mRNA levels of *Slc8b1* (coding for NCLX) were significantly higher in maturation (~2-fold). To test whether NCLX function was more prominent in maturation, we stimulated the enamel cells with ATP in the presence of the NCLX inhibitor CGP-37157. Blocking NCLX affected $_{m}Ca^{2+}$ efflux in secretory and maturation cells as shown by the increase in the rhod2AM fluorescence in both. However, the retention of $_{m}Ca^{2+}$ was significantly higher in maturation cells indicating that NCLX activity was more prominent at that stage, possibly explaining why the uptake by mitochondria of the Ca^{2+} bolus released from the ER appeared to be similar in both cell types.

ER-mitochondria Ca^{2+} exchanges are a restricted phenomenon that depends on the physical proximity of these two organelles. A different scenario is probing the responses of the mitochondria when global $_{c}Ca^{2+}$ changes take place such as when the Ca^{2+} fluxes are mediated by SOCE. We have shown that stimulation of SOCE in fura2AM loaded secretory and maturation ameloblasts results in an average SOCE peak of ~215 nM and ~590 nM, respectively (6, 15). Therefore, we investigated whether $_{m}Ca^{2+}$ uptake differed in enamel cells following the activation of SOCE. First, we analyzed the expression levels of genes associated with the MCU complex and its regulators. Only the expression of *Mcur1*, a positive modulator of MCU, was upregulated during maturation, with no changes in expression identified in *Mcu, Mcub, Micu1* or *Micu2.* Next, we tested the efficacy of the MCU blocker Ru265 (67) using the enamel cell line LS8 cells. As previously reported (67), we found that Ru265 was most effective when used at 50 μM in intact cells, and that this concentration did not affect the $\Delta\Psi m$. To address more directly if Ru265 blocked

$_{m}Ca^{2+}$, we permeabilized the LS8 cells and analyzed Ca^{2+} clearance after the application of several boluses of 20 μM of Ca^{2+} in the presence of Ru265 and RuR. We showed that both inhibitors prevented Ca^{2+} clearance.

Having addressed the efficacy of Ru265, we then induced SOCE using the SERCA inhibitor thapsigargin in secretory and maturation ameloblasts loaded with fluo4AM and rhod2AM to obtain simultaneous recordings of $_{c}Ca^{2+}$ and $_{m}Ca^{2+}$, respectively. We showed that $_{c}Ca^{2+}$ significantly increased in maturation stage ameloblasts as compared to secretory cells, as we had reported (5, 6, 15). In response to SOCE stimulation, we showed that the mitochondria of both cell types are capable of sequestering Ca^{2+}. However, maturation stage ameloblasts showed significantly higher rate of Ca^{2+} uptake and total amount of Ca^{2+} accumulated in the mitochondria. This is consistent with the MCU response to higher $_{c}Ca^{2+}$ loads.

The data presented here highlights several important features of mitochondria in ameloblast Ca^{2+} physiology. These mitochondria can sequester the Ca^{2+} pools released by the ER and the more global Ca^{2+} fluxes from the extracellular space. Addressing differences between stages, we found that the capacity of secretory and maturation stage ameloblasts to accumulate Ca^{2+} or when probed to sequester the Ca^{2+} bolus released by the ER are comparable. One of the main differences was the release of $_{m}Ca^{2+}$ by NCLX which appears to be more prominent in maturation, suggesting that maturation stage mitochondria are more dynamic in their capacity to dissipate $_{m}Ca^{2+}$, an important mechanism that helps prevent $_{m}Ca^{2+}$ overload (76).

Maturation stage ameloblasts are the main cell type involved in the mineralization of the enamel crystals and have an increased Ca^{2+} transport capacity overall (7, 77). This likely requires higher Ca^{2+} uptake, which we suggest is largely provided by SOCE which we estimated to be ~3-fold higher in maturation than in secretory ameloblasts (6). Therefore, maturation stage mitochondria help buffer Ca^{2+} uptake via SOCE.

The data shown here and in recent reports (23, 52) provide a picture of the physiological role of mitochondria in enamel mineralization. Maturation ameloblasts are metabolically more active and produce more ATP than secretory cells (23). The higher levels of ATP produced in maturation goes hand in hand with the overall increase in expression of ATP-dependent channels (e.g. CFTR) and pumps (e.g. SERCA) (18, 78, 79). For example, protein levels of SERCA, likely one of the most active consumers of ATP, were 3-fold higher in maturation (78). Ameloblast mitochondria also function as important Ca^{2+} buffers particularly in response to SOCE. This task is likely important to help prevent toxic levels of $_{c}Ca^{2+}$. Therefore, results shown here and in our previous study (23) suggest that mitochondria play a dual and significant role in enamel mineralization by supplying high levels of ATP and differentially buffering the Ca^{2+} fluxes via SOCE, advancing the notion that SOCE and $_{m}Ca^{2+}$ uptake are complementary processes in biological mineralization.

Supplementary Material

Refer to Web version on PubMed Central for supplementary material.

ACKONWLEDGEMENTS

The work presented here was funded by the National Institutes for Dental and Craniofacial Research (NICDR) grants DE025639 and DE027679 to RSL, MIUR PRIN 2017FS5SHL "RADIUS" grant to MG, National Institute of General Medical Sciences (NIGMS) grant GM115570 to EP. We thank Justin Wilson for kindly sharing the MCU blocker Ru265.

List of abbreviations:

ATP	adenosine triphosphate
$_{c}Ca^{2+}$	cytosolic Ca^{2+}
ER	endoplasmic reticulum
FCCP	Trifluoromethoxy carbonylcyanide phenylhydrazone
$_{m}Ca^{2+}$	Mitochondrial Ca^{2+}
Mat	maturation
Sec	secretory
MCU	mitochondrial Ca^{2+} uniporter
NCLX	Na^{+}-Li^{+}-Ca^{2+} exchanger
OXPHOS	oxidative phosphorylation
Ru265	Ruthenium 265
RuR	Ruthenium Red
SERCA	sarco/endoplasmic reticulum Ca^{2+}-ATPase
SOCE	store operated Ca^{2+} entry

REFERENCES

1. Smith CE (1998) Cellular and chemical events during enamel maturation. Crit Rev Oral Biol Med 9, 128–161 [PubMed: 9603233]
2. Lacruz RS, Smith CE, Bringas P Jr., Chen YB, Smith SM, Snead ML, Kurtz I, Hacia JG, Hubbard MJ, and Paine ML (2012) Identification of novel candidate genes involved in mineralization of dental enamel by genome-wide transcript profiling. J Cell Physiol 227, 2264–2275 [PubMed: 21809343]
3. Lacruz RS, Habelitz S, Wright JT, and Paine ML (2017) Dental Enamel Formation and Implications for Oral Health and Disease. Physiol Rev 97, 939–993 [PubMed: 28468833]
4. Bawden JW (1989) Calcium transport during mineralization. Anat Rec 224, 226–233 [PubMed: 2672887]
5. Nurbaeva MK, Eckstein M, Concepcion AR, Smith CE, Srikanth S, Paine ML, Gwack Y, Hubbard MJ, Feske S, and Lacruz RS (2015) Dental enamel cells express functional SOCE channels. Sci Rep 5, 15803 [PubMed: 26515404]
6. Nurbaeva MK, Eckstein M, Devotta A, Saint-Jeannet JP, Yule DI, Hubbard MJ, and Lacruz RS (2018) Evidence That Calcium Entry Into Calcium-Transporting Dental Enamel Cells Is Regulated by Cholecystokinin, Acetylcholine and ATP. Front Physiol 9, 801 [PubMed: 30013487]

7. Nurbaeva MK, Eckstein M, Feske S, and Lacruz RS (2016) Ca2+ transport and signalling in enamel cells. J Physiol
8. Nurbaeva MK, Eckstein M, Snead ML, Feske S, and Lacruz RS (2015) Store-operated Ca2+ Entry Modulates the Expression of Enamel Genes. J Dent Res 94, 1471–1477 [PubMed: 26232387]
9. Eckstein M, Vaeth M, Aulestia FJ, Costiniti V, Kassam SN, Bromage TG, Pedersen P, Issekutz T, Idaghdour Y, Moursi AM, Feske S, and Lacruz RS (2019) Differential regulation of Ca(2+) influx by ORAI channels mediates enamel mineralization. Sci Signal 12
10. Eckstein M, Vaeth M, Fornai C, Vinu M, Bromage TG, Nurbaeva MK, Sorge JL, Coelho PG, Idaghdour Y, Feske S, and Lacruz RS (2017) Store-operated Ca(2+) entry controls ameloblast cell function and enamel development. JCI Insight 2, e91166 [PubMed: 28352661]
11. Feske S, Gwack Y, Prakriya M, Srikanth S, Puppel SH, Tanasa B, Hogan PG, Lewis RS, Daly M, and Rao A (2006) A mutation in Orai1 causes immune deficiency by abrogating CRAC channel function. Nature 441, 179–185 [PubMed: 16582901]
12. Prakriya M, Feske S, Gwack Y, Srikanth S, Rao A, and Hogan PG (2006) Orai1 is an essential pore subunit of the CRAC channel. Nature 443, 230–233 [PubMed: 16921383]
13. Prakriya M, and Lewis RS (2015) Store-Operated Calcium Channels. Physiol Rev 95, 1383–1436 [PubMed: 26400989]
14. Putney JW (2011) The physiological function of store-operated calcium entry. Neurochemical research 36, 1157–1165 [PubMed: 21234676]
15. Bomfim GHS, Costiniti V, Li Y, Idaghdour Y, and Lacruz RS (2020) TRPM7 activation potentiates SOCE in enamel cells but requires ORAI. Cell Calcium 87
16. Paine ML, Boyde A, and Lacruz RS (2020) Transport Functions of Ectoderm Epithelial Cells Forming Dental Enamel. In Ion Transport Across Epithelial Tissues and Disease (DC H. K. a. D., ed), Springer
17. Lacruz RS (2017) Enamel: Molecular identity of its transepithelial ion transport system. Cell Calcium 65, 1–7 [PubMed: 28389033]
18. Lacruz RS, Habelitz S, Wright JT, and Paine ML (2017) Dental Enamel Formation and Implications for Oral Health and Disease. Physiological Reviews 97, 939–993 [PubMed: 28468833]
19. Eckstein M, and Lacruz RS (2018) CRAC channels in dental enamel cells. Cell Calcium 75, 14–20 [PubMed: 30114531]
20. Malli R, Frieden M, Osibow K, Zoratti C, Mayer M, Demaurex N, and Graier WF (2003) Sustained Ca2+ transfer across mitochondria is Essential for mitochondrial Ca2+ buffering, sore-operated Ca2+ entry, and Ca2+ store refilling. J Biol Chem 278, 44769–44779 [PubMed: 12941956]
21. Demaurex N, and Guido D (2017) The Role of Mitochondria in the Activation/Maintenance of SOCE: Membrane Contact Sites as Signaling Hubs Sustaining Store-Operated Ca(2+) Entry. Adv Exp Med Biol 993, 277–296 [PubMed: 28900920]
22. Hoth M, Fanger CM, and Lewis RS (1997) Mitochondrial regulation of store-operated calcium signaling in T lymphocytes. J Cell Biol 137, 633–648 [PubMed: 9151670]
23. Costiniti V, Bomfim GH, Li Y, Mitaishvili E, Ye Z.-w., Zhang J, Townsend DM, Giacomello M, and Lacruz RS (2020) Mitochondrial Function in Enamel Development. Frontiers in physiology 11
24. Lehninger AL, Nelson DL, and Cox MM (2003) Principles of Biochemistry. Bologna: Zanichelli
25. Jouaville LS, Pinton P, Bastianutto C, Rutter GA, and Rizzuto R (1999) Regulation of mitochondrial ATP synthesis by calcium: evidence for a long-term metabolic priming. Proc Natl Acad Sci U S A 96, 13807–13812 [PubMed: 10570154]
26. Shanmughapriya S, Rajan S, Hoffman NE, Zhang X, Guo S, Kolesar JE, Hines KJ, Ragheb J, Jog NR, Caricchio R, Baba Y, Zhou Y, Kaufman BA, Cheung JY, Kurosaki T, Gill DL, and Madesh M (2015) Ca2+ signals regulate mitochondrial metabolism by stimulating CREB-mediated expression of the mitochondrial Ca2+ uniporter gene MCU. Sci Signal 8, ra23 [PubMed: 25737585]
27. Rizzuto R, De Stefani D, Raffaello A, and Mammucari C (2012) Mitochondria as sensors and regulators of calcium signalling. Nat Rev Mol Cell Biol 13, 566–578 [PubMed: 22850819]

28. Rizzuto R, Bernardi P, and Pozzan T (2000) Mitochondria as all-round players of the calcium game. J Physiol 529 Pt 1, 37–47 [PubMed: 11080249]
29. Giacomello M, Drago I, Pizzo P, and Pozzan T (2007) Mitochondrial Ca2+ as a key regulator of cell life and death. Cell Death Differ 14, 1267–1274 [PubMed: 17431419]
30. Drago I, De Stefani D, Rizzuto R, and Pozzan T (2012) Mitochondrial Ca2+ uptake contributes to buffering cytoplasmic Ca2+ peaks in cardiomyocytes. Proc Natl Acad Sci U S A 109, 12986–12991 [PubMed: 22822213]
31. Pozzan T, Magalhaes P, and Rizzuto R (2000) The comeback of mitochondria to calcium signalling. Cell calcium 28, 279–283 [PubMed: 11115367]
32. Granatiero V, De Stefani D, and Rizzuto R (2017) Mitochondrial Calcium Handling in Physiology and Disease. Adv Exp Med Biol 982, 25–47 [PubMed: 28551780]
33. Tarasov AI, Semplici F, Ravier MA, Bellomo EA, Pullen TJ, Gilon P, Sekler I, Rizzuto R, and Rutter GA (2012) The mitochondrial Ca2+ uniporter MCU is essential for glucose-induced ATP increases in pancreatic beta-cells. PloS one 7, e39722 [PubMed: 22829870]
34. De Stefani D, Rizzuto R, and Pozzan T (2016) Enjoy the Trip: Calcium in Mitochondria Back and Forth. Annu Rev Biochem 85, 161–192 [PubMed: 27145841]
35. Baughman JM, Perocchi F, Girgis HS, Plovanich M, Belcher-Timme CA, Sancak Y, Bao XR, Strittmatter L, Goldberger O, Bogorad RL, Koteliansky V, and Mootha VK (2011) Integrative genomics identifies MCU as an essential component of the mitochondrial calcium uniporter. Nature 476, 341–345 [PubMed: 21685886]
36. De Stefani D, Raffaello A, Teardo E, Szabo I, and Rizzuto R (2011) A forty-kilodalton protein of the inner membrane is the mitochondrial calcium uniporter. Nature 476, 336–340 [PubMed: 21685888]
37. Mallilankaraman K, Cardenas C, Doonan PJ, Chandramoorthy HC, Irrinki KM, Golenar T, Csordas G, Madireddi P, Yang J, Muller M, Miller R, Kolesar JE, Molgo J, Kaufman B, Hajnoczky G, Foskett JK, and Madesh M (2015) MCUR1 is an essential component of mitochondrial Ca(2+) uptake that regulates cellular metabolism. Nat Cell Biol 17, 953
38. Doonan PJ, Chandramoorthy HC, Hoffman NE, Zhang X, Cardenas C, Shanmughapriya S, Rajan S, Vallem S, Chen X, Foskett JK, Cheung JY, Houser SR, and Madesh M (2014) LETM1-dependent mitochondrial Ca2+ flux modulates cellular bioenergetics and proliferation. FASEB J 28, 4936–4949 [PubMed: 25077561]
39. Vais H, Mallilankaraman K, Mak DD, Hoff H, Payne R, Tanis JE, and Foskett JK (2016) EMRE Is a Matrix Ca(2+) Sensor that Governs Gatekeeping of the Mitochondrial Ca(2+) Uniporter. Cell Rep 14, 403–410 [PubMed: 26774479]
40. Mallilankaraman K, Doonan P, Cardenas C, Chandramoorthy HC, Muller M, Miller R, Hoffman NE, Gandhirajan RK, Molgo J, Birnbaum MJ, Rothberg BS, Mak DO, Foskett JK, and Madesh M (2012) MICU1 is an essential gatekeeper for MCU-mediated mitochondrial Ca(2+) uptake that regulates cell survival. Cell 151, 630–644 [PubMed: 23101630]
41. Foskett JK, and Philipson B (2015) The mitochondrial Ca(2+) uniporter complex. J Mol Cell Cardiol 78, 3–8 [PubMed: 25463276]
42. Carvalho EJ, Stathopulos PB, and Madesh M (2020) Regulation of Ca(2+) exchanges and signaling in mitochondria. Curr Opin Physiol 17, 197–206 [PubMed: 33103015]
43. Murgia M, and Rizzuto R (2015) Molecular diversity and pleiotropic role of the mitochondrial calcium uniporter. Cell Calcium 58, 11–17 [PubMed: 26048007]
44. De Stefani D, Patron M, and Rizzuto R (2015) Structure and function of the mitochondrial calcium uniporter complex. Biochim Biophys Acta 1853, 2006–2011 [PubMed: 25896525]
45. Rizzuto R, and Pozzan T (2006) Microdomains of intracellular Ca2+: molecular determinants and functional consequences. Physiol Rev 86, 369–408 [PubMed: 16371601]
46. Palty R, Silverman WF, Hershfinkel M, Caporale T, Sensi SL, Parnis J, Nolte C, Fishman D, Shoshan-Barmatz V, Herrmann S, Khananshvili D, and Sekler I (2010) NCLX is an essential component of mitochondrial Na+/Ca2+ exchange. Proc Natl Acad Sci U S A 107, 436–441 [PubMed: 20018762]
47. De Marchi U, Santo-Domingo J, Castelbou C, Sekler I, Wiederkehr A, and Demaurex N (2014) NCLX protein, but not LETM1, mediates mitochondrial Ca2+ extrusion, thereby limiting Ca2+-

induced NAD(P)H production and modulating matrix redox state. J Biol Chem 289, 20377–20385 [PubMed: 24898248]

48. Takano Y, Yamamoto T, Domon T, and Wakita M (1990) Histochemical, ultrastructural, and electron microprobe analytical studies on the localization of calcium in rat incisor ameloblasts at early stage amelogenesis. Anat Rec 228, 123–131 [PubMed: 2240606]
49. Hubbard MJ, and McHugh NJ (1996) Mitochondrial ATP synthase F1-beta-subunit is a calcium-binding protein. FEBS Lett 391, 323–329 [PubMed: 8764999]
50. Josephsen K, and Fejerskov O (1977) Ameloblast modulation in the maturation zone of the rat incisor enamel organ. A light and electron microscopic study. J Anat 124, 45–70 [PubMed: 914705]
51. Costiniti V, Bomfim GH, Li Y, Mitaishvili E, Ye Z-W, Zhang J, Townsend DM, Giacomello M, and Lacruz RS (2020) Mitochondrial function in enamel development. Frontiers in physiology
52. Imhof T, Rosenblatt K, Pryymachuk G, Weiland D, Noetzel N, Deschner J, Baris OR, Kimoloi S, Koch M, Wiesner RJ, and Korkmaz Y (2020) Epithelial loss of mitochondrial oxidative phosphorylation leads to disturbed enamel and impaired dentin matrix formation in postnatal developed mouse incisor. Sci Rep 10, 22037 [PubMed: 33328493]
53. Rizzuto R, Duchen MR, and Pozzan T (2004) Flirting in little space: the ER/mitochondria Ca2+ liaison. Science's STKE : signal transduction knowledge environment 2004, re1
54. Lacruz RS (2017) Enamel: Molecular identity of its transepithelial ion transport system. Cell calcium
55. Chen LS , C. RI, Hsu D, Luo W, Snead ML (1992) Maintenance of Amelogenin Gene Expression by Transformed Epithelial Cells of Mouse Enamel Organ. 37, 771–778
56. Benz R, and McLaughlin S (1983) The molecular mechanism of action of the proton ionophore FCCP (carbonylcyanide p-trifluoromethoxyphenylhydrazone). Biophys J 41, 381–398 [PubMed: 6838976]
57. Aulestia FJ, Groeling J, Bomfim GHS, Costiniti V, Manikandan V, Chaloemtoem A, Concepcion AR, Li Y, Wagner LE 2nd, Idaghdour Y, Yule DI, and Lacruz RS (2020) Fluoride exposure alters Ca(2+) signaling and mitochondrial function in enamel cells. Sci Signal 13
58. Roy SS, and Hajnóczky G (2008) Calcium, mitochondria and apoptosis studied by fluorescence measurements. Methods 46, 213–223 [PubMed: 18948203]
59. Solesio ME, Garcia Del Molino LC, Elustondo PA, Diao C, Chang JC, and Pavlov EV (2020) Inorganic polyphosphate is required for sustained free mitochondrial calcium elevation, following calcium uptake. Cell calcium 86, 102127 [PubMed: 31954928]
60. Szabadkai G, and Duchen MR (2008) Mitochondria: the hub of cellular Ca2+ signaling. Physiology (Bethesda) 23, 84–94 [PubMed: 18400691]
61. Dimmer KS, and Scorrano L (2006) (De)constructing Mitochondria: What For? Physiology (Bethesda) 21, 233–241 [PubMed: 16868312]
62. Lehninger AL, Carafoli E, and Rossi CS (1967) Energy-linked ion movements in mitochondrial systems. Adv Enzymol Relat Areas Mol Biol 29, 259–320 [PubMed: 4881885]
63. Chalmers S, and Nicholls DG (2003) The relationship between free and total calcium concentrations in the matrix of liver and brain mitochondria. J Biol Chem 278, 19062–19070 [PubMed: 12660243]
64. Salter MW, and Hicks JL (1994) ATP-evoked increases in intracellular calcium in neurons and glia from the dorsal spinal cord. J Neurosci 14, 1563–1575 [PubMed: 8126555]
65. Salter MW, and Hicks JL (1995) ATP causes release of intracellular Ca2+ via the phospholipase C beta/IP3 pathway in astrocytes from the dorsal spinal cord. J Neurosci 15, 2961–2971 [PubMed: 7722640]
66. Cox DA, Conforti L, Sperelakis N, and Matlib MA (1993) Selectivity of inhibition of Na(+)-Ca2+ exchange of heart mitochondria by benzothiazepine CGP-37157. J Cardiovasc Pharmacol 21, 595–599 [PubMed: 7681905]
67. Woods JJ, Nemani N, Shanmughapriya S, Kumar A, Zhang M, Nathan SR, Thomas M, Carvalho E, Ramachandran K, Srikantan S, Stathopulos PB, Wilson JJ, and Madesh M (2019) A Selective and Cell-Permeable Mitochondrial Calcium Uniporter (MCU) Inhibitor Preserves

Mitochondrial Bioenergetics after Hypoxia/Reoxygenation Injury. ACS Cent Sci 5, 153–166 [PubMed: 30693334]

68. Woods JJ, Rodriguez MX, Tsai CW, Tsai MF, and Wilson JJ (2021) Cobalt amine complexes and Ru265 interact with the DIME region of the mitochondrial calcium uniporter. Chemical communications 57, 6161–6164 [PubMed: 34042919]
69. Sarkar J, Simanian EJ, Tuggy SY, Bartlett JD, Snead ML, Sugiyama T, and Paine ML (2014) Comparison of two mouse ameloblast-like cell lines for enamel-specific gene expression. Front Physiol 5, 277 [PubMed: 25120490]
70. Mallilankaraman K, Cardenas C, Doonan PJ, Chandramoorthy HC, Irrinki KM, Golenar T, Csordas G, Madireddi P, Yang J, Muller M, Miller R, Kolesar JE, Molgo J, Kaufman B, Hajnoczky G, Foskett JK, and Madesh M (2012) MCUR1 is an essential component of mitochondrial Ca2+ uptake that regulates cellular metabolism. Nat Cell Biol 14, 1336–1343 [PubMed: 23178883]
71. Ambudkar IS, de Souza LB, and Ong HL (2017) TRPC1, Orai1, and STIM1 in SOCE: Friends in tight spaces. Cell calcium 63, 33–39 [PubMed: 28089266]
72. Plachot JJ, Thil CL, Enault G, Halpern S, Cournot-Witmer G, and Balsan S (1986) Mitochondrial calcium and bone mineralization in the rat fetus. Bone Miner 1, 157–166 [PubMed: 3508723]
73. Dobson PF, Dennis EP, Hipps D, Reeve A, Laude A, Bradshaw C, Stamp C, Smith A, Deehan DJ, Turnbull DM, and Greaves LC (2020) Mitochondrial dysfunction impairs osteogenesis, increases osteoclast activity, and accelerates age related bone loss. Sci Rep 10, 11643 [PubMed: 32669663]
74. Halstead LB (1969) Are mitochondria directly involved in biological mineralisation? The mitochondrion and the origin of bone. Calcif Tissue Res 3, 103–105 [PubMed: 5814431]
75. Shapiro IM, and Greenspan JS (1969) Are mitochondria directly involved in biological mineralisation? Calcif Tissue Res 3, 100–102 [PubMed: 5772443]
76. Stephanopoulos G, Garefalaki ME, and Lyroudia K (2005) Genes and related proteins involved in amelogenesis imperfecta. J Dent Res 84, 1117–1126 [PubMed: 16304440]
77. Hubbard MJ (2000) Calcium transport across the dental enamel epithelium. Crit Rev Oral Biol Med 11, 437–466 [PubMed: 11132765]
78. Franklin IK, Winz RA, and Hubbard MJ (2001) Endoplasmic reticulum Ca2+-ATPase pump is up-regulated in calcium-transporting dental enamel cells: a non-housekeeping role for SERCA2b. Biochem J 358, 217–224 [PubMed: 11485570]
79. Lacruz RS, Smith CE, Moffatt P, Chang EH, Bromage TG, Bringas P Jr., Nanci A, Baniwal SK, Zabner J, Welsh MJ, Kurtz I, and Paine ML (2012) Requirements for ion and solute transport, and pH regulation during enamel maturation. J Cell Physiol 227, 1776–1785 [PubMed: 21732355]

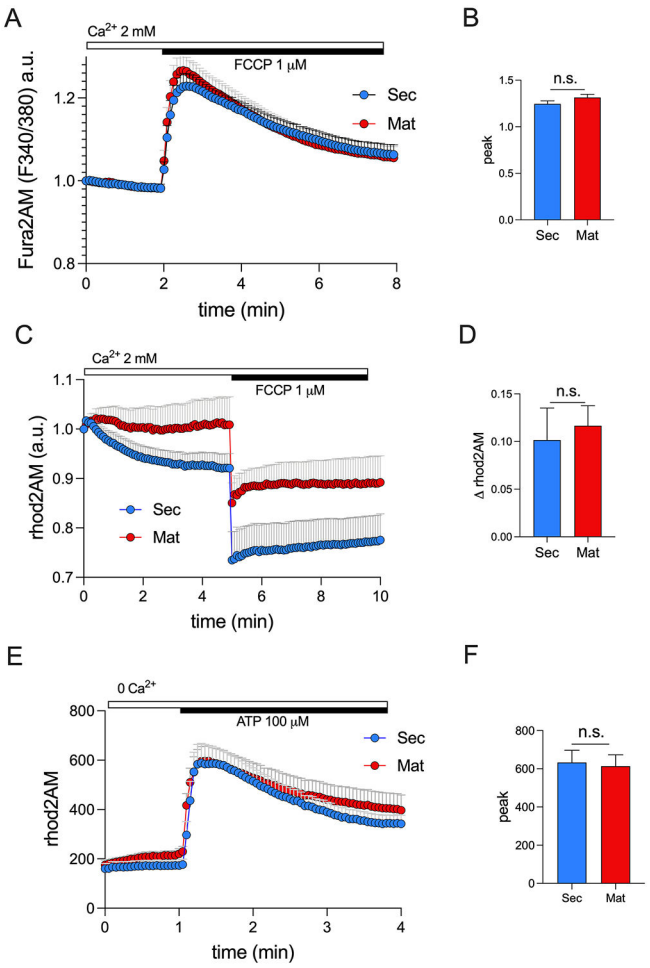

Figure 1: Quantification of mitochondrial Ca^{2+} dynamics in ameloblasts.

A) Original traces of secretory and maturation ameloblasts loaded with the cytosolic Ca^{2+} indicator fura2AM (1 µM) stimulated with FCCP (1 µM). **B)** Quantification of Ca^{2+} peak. **C)** Original traces of secretory and maturation ameloblasts loaded with the mitochondrial Ca^{2+} indicator rhod2AM (4 µM) stimulated with FCCP (1 µM). **D)** Quantification of rhod2AM delta (Δ). **E)** Original traces of secretory and maturation ameloblasts loaded with rhod2AM and stimulated with ATP (100 µM). **F)** Quantification of Ca^{2+} peak. For A, C and E, data represent the mean ± SEM of n = 6 independent experiments, 3 slides for each condition 20 - 100 cells per field. Data were analyzed by 2 - tailed unpaired Student's t test. n.s., non-significant.

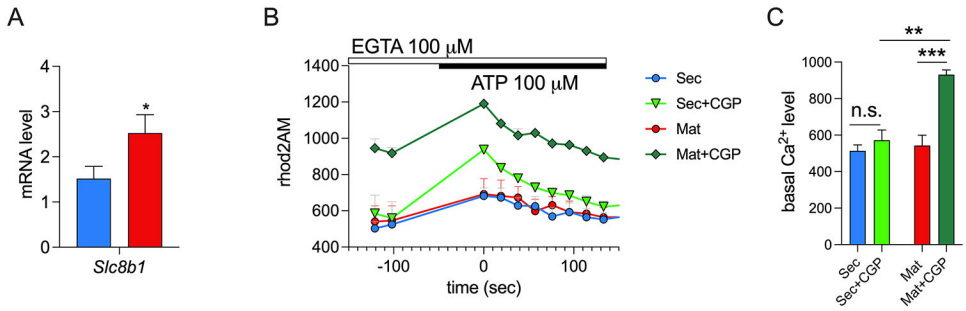

Figure 2: NCLX expression and function in ameloblasts.

A) mRNA expression of *Slc8b1* (coding for NCLX) in secretory and maturation stage ameloblasts (n = 6 animals). **B)** Original traces showing mitochondrial Ca^{2+} accumulation in secretory and maturation stage ameloblasts loaded with the mitochondrial Ca^{2+} indicator rhod2AM (4 μM) in the presence/absence of the NCLX inhibitor CGP-37157 (10 μM). **C)** Quantification of the Ca^{2+} basal level. Data represent the mean ± SEM of 3 independent experiments, 4 wells for each condition with 20-50 cells per field. Data were analyzed by 2 - tailed unpaired Student's t test and one-way ANOVA. $^{**}P < 0.01$, $^{***}P < 0.001$, n.s., non-significant.

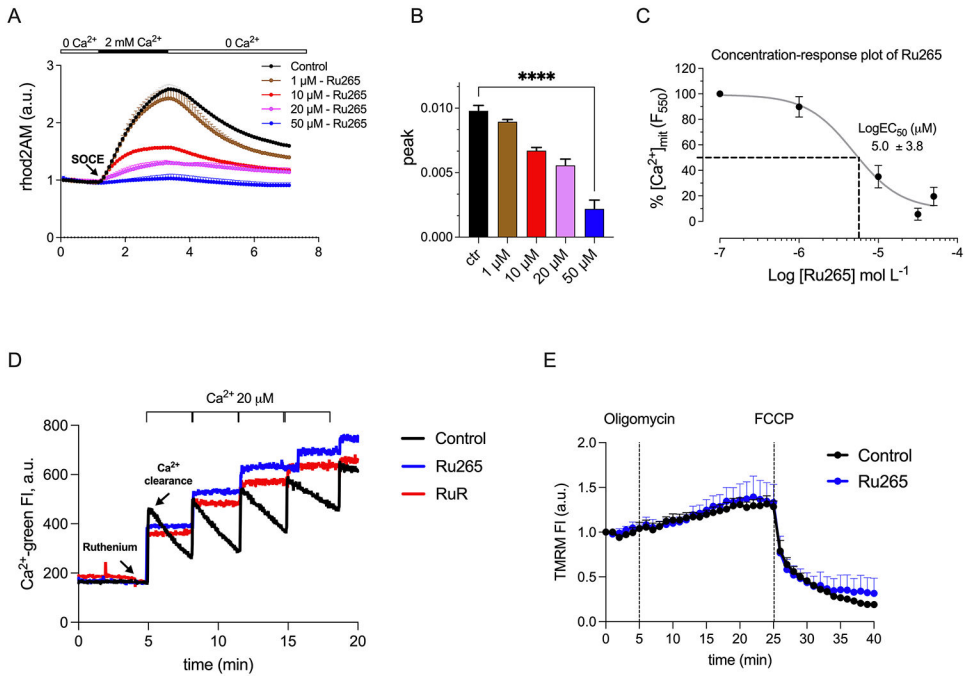

Figure 3: Efficiency of the MCU blocker Ru265 in LS8 enamel cells.

A-B) Quantification of mitochondrial Ca^{2+} uptake in rhod2AM (4 µM) loaded LS8 cells (~120 cells/field per condition) treated with Ru265 for 1 h at the following concentrations: 1, 10, 20 and 50 µM. Data were analyzed by one-way ANOVA. ****$P < 0.0001$ **C)** $LogEC_{50}$ plot for data in A and B. **D)** Quantification of Ca^{2+} clearance in digitonin-permeabilized LS8 cells (n = 800 K cells) loaded with Calcium Green-5 N (1 µM) in the presence of Ru265 (5 µM) or RuR (5 µM) after the application of Ca^{2+} boluses (20 µM). **E)** Mitochondrial membrane potential (ΔΨm) measured using TMRM (40 nM) in LS8 cells (n = 200 K). Oligomycin A (5 µM) and FCCP (5 µM) were added to the cells to induce mitochondria hyper- and depolarization, respectively. Data represent mean ± SEM, from a minimum of 3 independent experiments.

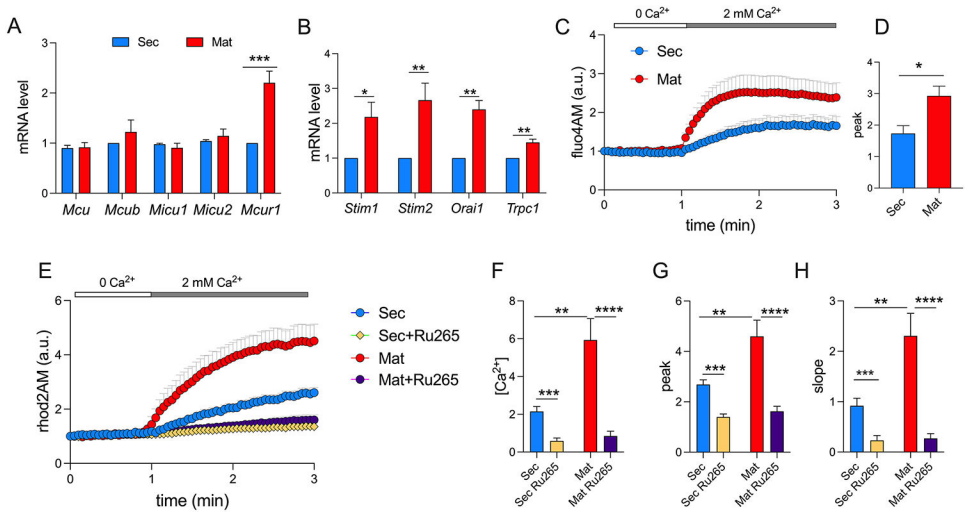

Figure 4: Mitochondrial Ca^{2+} uptake in ameloblasts.

A) Quantification of mRNA levels by RT-qPCR of genes associated with the mitochondrial uniporter complex components and **B)** with SOCE in secretory and maturation ameloblasts (n = 10 animals). Data were analyzed by 2 - tailed unpaired Student's t test. *$P < 0.05$, **$P < 0.01$, ***$P < 0.001$. **C)** Original traces of SOCE in fluo4AM (1 μM) loaded secretory and maturation ameloblasts stimulated with thapsigargin (2 μM). **D)** Quantification of Ca^{2+} peak of data in **C**. **E)** Original traces of secretory and maturation ameloblasts loaded with rhod2AM (4 μM) stimulated with thapsigargin (2 μM) in the presence/absence of the MCU blocker Ru265 (50 μM). **F-H)** Quantification of area under the curve, Ca^{2+} peak and slope of data in **E**. A minimum of ~100 cells per condition were used. Data represent the mean ± SEM of 4 independent experiments. Data were analyzed by one-way ANOVA and 2 - tailed unpaired Student's t test. *$P < 0.05$, **$P < 0.01$, ***$P < 0.001$ or ****$P < 0.0001$.

Table 1:

Primer sequences used for RT-qPCR.

Rat Primers		
Gene	**Forward Sequence**	**Reverse Sequence**
β-Actin	CACACTGTGCCCATCTATGA	CCGATAGTGATGACCTGACC
Enam	TGCAGAAATACAGCTTCTCCT	CATTGGCATTGGCATGGCA
Mcu	CCAGTTCACACTCAAGCCTATC	CAGCAACTCGAACACCATCT
Mcub	CATGTAACTCGGCAGAACT	GCTGACTTCCTGTCCTTGAA
Mcur1	AATAGTGTCCCTGCATGCCC	AGGCGGTAAAATCCCAGAGC
Micu1	AATCAACGAACCTGGTGAAA	GTGTTCTGGCTGCTTCTCAT
Micu2	CGCTGACTCGGTAATGTCTT	TTCCCTGGTGGACTTGTTTA
Odam	ATCAATTTGGATTTGTACCACA	CGTCGGGTTTATTTCAGAAGTGA
Orai1	GGTGAAGTTCTTACCGCTCA	ACGGCAAAGACGATAAACAC
Slc8b1	CTGGGCCTCTATGTCTTCTATG	GTAGCTCTGGTGTCTCTGATATG
Stim1	CTGTCTCTGCTGTCCCAGTT	TCCATAGAACAATCCCCAGA
Stim2	ATGCACCAGCTCTCTAGTGG	TTGATGGCTTTTTGCTTTTC
Trpc1	TTCCAAAGAGCAGAAGGACTG	AGGTGCCAATGAACGAGTG